A Control-oriented Model for Trajectory-based HCCI Combustion Control

Zhang, Chen
University of Minnesota, Twin-cites Campus
111 Church Street SE, ME 452, Minneapolis, MN, 55455
zhan2314@umn.edu

Sun, Zongxuan[1]
University of Minnesota, Twin-cites Campus
111 Church Street SE, ME 3110, Minneapolis, MN, 55455
zsun@umn.edu

ABSTRACT

Previously, the authors have proposed the concept of piston trajectory-based HCCI combustion control enabled by a free piston engine and shown its benefits on both engine thermal efficiency and emissions by implementing various piston trajectories. In order to realize the HCCI trajectory-based combustion control in practical applications, a control-oriented model with sufficient chemical kinetics information has to be developed. In this paper, such a model is proposed and its performance, in terms of computational speed and model fidelity, are compared to three existing models: a simplified model using a one-step global reaction, a reduced-order model using Jones-Lindstedt mechanism and a complex physics-based model including detailed chemical reaction mechanisms. A unique phase separation method is proposed to significantly reduce the computational time and guarantee the prediction accuracy simultaneously. In addition,

---

The material in this paper was partially presented at the 2015 American Control Conference, July 1-3, Chicago, IL [46]. A new phase separation method, more detailed analysis of the model at various working conditions and using the model for HCCI combustion phasing control during transient operations are presented in this paper.

[1] Corresponding author, Tel. 612-625-2107

the paper also shows that the high fidelity of the proposed model is sustained at multiple working conditions, including different air-fuel ratios, various compression ratios and distinct piston motion patterns between the two end positions. Finally, an example is presented showing how the control-oriented model enables real time optimization of the HCCI combustion phasing by varying the trajectories. The simulation results show that the combustion phasing can be adjusted quickly as desired, which further demonstrates the effectiveness of the piston trajectory-based combustion control.

Keywords*: control-oriented model, free piston engine, trajectory-based combustion control, phase separation method*

INTRODUCTION

A key challenge for a sustainably transportation system is to reduce automotive fuel consumption and emissions. Homogeneous charge compression ignition (HCCI) combustion was proposed to overcome this challenge. The extensive studies have shown that the HCCI combustion is able to improve the fuel economy as well as engine emissions due to its shorter combustion duration, higher available compression ratio (CR) and lower combustion temperature [1-3]. However, the HCCI combustion has yet to be realized in mass production, mainly due to the lack of adequate control means in the conventional internal combustion engine (ICE) to adjust the HCCI combustion over the entire operating range. As shown in Fig. 1, the HCCI combustion process is determined by the interaction between the chemical kinetics and the in-cylinder gas dynamics in a feedback manner. The existing control methods in conventional engines, such as regulating exhaust gas recirculation [4-6], variable valve timings [7-9] and stratifying

charge [10, 11], can only influence the dynamic interaction cycle-by-cycle, rather than adjust it in real-time. Therefore, the existing control methods have a limited effect on regulating the complete combustion process.

A novel control method, namely trajectory-based combustion control, was then proposed by the authors, which provides a new framework to control the HCCI combustion or other low temperature combustion mode [12-14]. This method is enabled by the free piston engine (FPE) architecture, whose piston motion is not constrained by the mechanical crankshaft [15, 16]. This extra degree of freedom of the piston enables significant benefits of the FPE, such as variable CR and higher thermal efficiency. However, it also raises a challenges on piston motion control, which forms the main technical barrier for the wide-spread of the FPE. Previously, an active piston motion control, named as “virtual crankshaft”, was designed and verified experimentally [15]. The control method coordinates the in-cylinder gas forces and loading forces in real-time and regulates the piston following a desired reference precisely [15, 17]. As a result, the piston trajectory becomes an active control variable, which can be manipulated in real-time to regulate the combustion chamber volume and therefore adjust the gas pressure-temperature history and species concentration prior, during, and after the combustion event (Fig. 1). The effectiveness of this control method has been demonstrated by the simulation studies of a comprehensive physical-based model with detailed reaction mechanisms of various fuels [12-14].

Under such a new framework, the extra degree of freedom of the piston trajectory not only realizes the real-time control of the HCCI combustion, but also enables the

optimization of the related chemical reactivity and heat transfer processes [18]. Nonetheless, the detailed physical-based model is not suitable for the control purpose. The detailed reaction mechanisms usually consist of hundreds of species and thousands of reactions and the related models therefore possess heavy computational burden, even under the assumption of homogeneous environment. Meanwhile, the large amount of species in the detailed mechanisms also increases the order of the dynamic model and causes significant challenge for the subsequent optimization. Extensive studies have been conducted to reduce the order of combustion reaction mechanisms through sensitivity analysis and reaction rate analysis (such as principal component analysis) [19, 20], intrinsic low-dimensional manifolds [21], computational singular perturbation [22], directed relation graph [23], and its derivative version, directed relation graph with error propagation [24]. However, the corresponding reaction mechanisms, or the so-called skeleton mechanisms with several species and tens of reactions, are still mainly utilized for offline simulation rather than real time control due to the relatively long turnaround time [25-29].

On the other hand, existing HCCI control-oriented models usually assume engine's compression and expansion strokes are polytropic, and employ empirical correlations, e.g. temperature thresholds or integral of Arrhenius equations, to predict the start of combustion (SOC) [30-35]. In addition, the heat release of the HCCI combustion is either assumed as an instantaneous process [30] or simulated via Wiebe function [31-35]. Even though the computational cost is decreased significantly, these assumptions over-simplify the utilized chemical kinetics. Considering the fact that the HCCI combustion is

mainly driven by the chemical kinetics, the existing control-oriented models lack the necessary information to predict the dynamics of the combustion process and the emissions production.

Therefore, in order to implement the piston trajectory-based HCCI combustion control in real-time and achieve the optimization of piston trajectory according to variable working conditions, a new control-oriented model with short computation time and sufficient chemical kinetic information is needed. Such a model is proposed in this paper. The rest of the paper is organized as follow: The detailed modeling approach is described in section II. The simulation results of the proposed model at multiple working conditions, as well as the comparison with a simplified model, a reduced order model with Jones-Lindstet reaction mechanism and a complex model with detailed reaction mechanisms, are investigated in section III. An example showing how to use the proposed model regulating the HCCI combustion phasing in real time through the variable piston trajectories is also presented in section III. Finally, the advantages of the proposed model are concluded in section IV.

MODELING APPROACH

The proposed control-oriented model consists of three components. First, a new mechanism producing variable piston trajectories is introduced. Unlike slider-crank mechanism [36], the new mechanism adds an additional degree of freedom to the piston motion and represents the unique characteristic of the FPE. Secondly, a physics-based model is developed to describe the in-cylinder gas dynamics. In addition, a specific reaction mechanism is also employed to represent the chemical kinetics of the

fuels. It is worth mentioning that a unique phase separation method is proposed while developing the reaction mechanism, aimed to reduce the computational cost and sustain sufficient chemical information simultaneously.

A. Variable Piston Trajectories

Unlike the conventional ICE, the FPE has no constraints on its piston motion due to the absence of the mechanical crankshaft mechanism. As a result, variable piston trajectories with different CRs and motion patterns between the bottom dead center (BDC) and the top dead center (TDC) can be easily achieved in a FPE. Hence the conventional slider-crank mechanism is inappropriate to describe these piston trajectories and a new mechanism is needed to represent the piston motion. In this paper, the FPE piston trajectory is represented as the x-axis displacement of a point moving around an ellipse in the Cartesian coordinate, as shown in Fig. 2.

The corresponding piston trajectories *S* can be yielded as:

$$S = \frac{A \cdot \Omega \cdot \cos(2\pi f \cdot t)}{\sqrt{\Omega^2 \cdot \cos(2\pi f \cdot t)^2 + \sin(2\pi f \cdot t)^2}} + B \tag{1}$$

where *A* is the major axis of the ellipse, *B* is the location of the ellipse center as the bias, *f* represents the frequency of the engine operation, *Ω* (= minor axis / major axis) implies the shape of the ellipse and *t* stands for the time.

Fig. 3 shows the corresponding results of piston trajectories with various CRs and different piston motion patterns between the TDC and BDC points. It has been shown that the FPE enables significant improvement on the thermal efficiency and reduction of

NOx emissions simultaneously by implementing appropriate piston trajectories accordingly [12-14].

B. Physics-based Model

The physics-based model is developed based on the first law of thermodynamics applied to a closed system, while the scavenging process is neglected. The states include pressure *P*, temperature *T* and each species concentration [X_i] inside the reaction mechanism. In this subsection, the rate equations of pressure *P* and temperature *T* are introduced, and the rates of each species concentrations [X_i] will be discussed in the next subsection.

1) Pressure rate equation

From the idea gas law, the pressure of the in-cylinder gas, *P,* and its time derivative can be represented as below: (*R* is the universal gas constant)

$$P = \sum_i [X_i] \cdot R \cdot T \tag{2}$$

$$\dot{P} = P \cdot \sum_i [\dot{X}_i] / \sum_i [X_i] + P \cdot \dot{T} / T \tag{3}$$

2) Temperature rate equation

In order to derive the rate equation for the in-cylinder gas temperature *T*, the first law of the thermodynamics for a closed system and the ideal gas law has to be combined as follow.

The first law of the thermodynamics for a closed system is:

$$\frac{d(mu)}{dt} = -\dot{Q} - \dot{W} \tag{4}$$

where m is the total mass in the cylinder, u is the specific internal energy of the in-cylinder gas, $\dot{Q}$ is the heat transfer rate and $\dot{W}$ is the expansion work rate.

Furthermore, the heat transfer process is assumed as a convection process:

$$\dot{Q} = h_{hl} \cdot A_{wall} \cdot (T - T_{wall}) \tag{5}$$

where T_{wall} is the wall temperature, A_{wall} is the heat transfer surface area and h_{hl} is the heat transfer coefficient, which is determined by a modified Woschini correlation [36]:

$$A_{wall} = 2 \cdot \frac{\pi}{4} \cdot b^2 + \alpha \cdot \pi \cdot b \cdot S \tag{6}$$

$$h_{hl} = 3.26 \cdot b^{-0.2} \cdot P^{0.8} \cdot T^{-0.55} \cdot w^{0.8} \tag{7}$$

In (6) and (7), b represents the bore of the engine, S is the piston trajectory, α is a FPE architecture parameter (= 2, when the FPE uses the opposed piston architecture) and w is the average in-cylinder gas velocity.

Besides, the rate of expansion work is obtained as [35, 36]:

$$\dot{W} = P \cdot \dot{V} \tag{8}$$

where V is the combustion chamber volume, which is determined by the piston trajectory S:

$$V = \frac{\pi}{4} \cdot b^2 \cdot \alpha \cdot S \tag{9}$$

Now, given the fact that the specific enthalpy h can be obtained from the specific internal energy u:

$$h = u + P \cdot v \tag{10}$$

where *v* is the specific volume of the in-cylinder gas.

Combining (4), (8) and (10), the following equation can be obtained:

$$\frac{d(m \cdot h)}{dt} = \dot{m} \cdot P \cdot v + \dot{P} \cdot V - \dot{Q} \tag{11}$$

Due to the closed system assumption, (11) can be further simplified as:

$$\frac{d(m \cdot h)}{dt} = \dot{P} \cdot V - \dot{Q} \tag{12}$$

On the other hand, the total enthalpy of the in-cylinder gas can also be derived via the sum of each species enthalpy:

$$m \cdot h = \sum_i N_i \cdot \hat{h}_i \tag{13}$$

where N_i is the moles number of species *i* and $\hat{h}_i$ is mole-based specific enthalpy of species *i*. Furthermore, the rate of $\hat{h}_i$ can be calculated as:

$$\dot{\hat{h}}_i = c_{p,i}(T) \cdot \dot{T} \tag{14}$$

where $c_{p,i}(T)$ is the mole-based constant pressure heat capacity of specie *i* at temperature *T*.

Therefore, the time differential of the total enthalpy is:

$$\begin{aligned} \frac{d(m \cdot h)}{dt} &= \sum_i (\frac{dN_i}{dt} \cdot \hat{h}_i) + \sum_i (\frac{d\hat{h}_i}{dt} \cdot N_i) \\ &= V \cdot \sum_i ([\dot{X}_i] \cdot \hat{h}_i) + \dot{V} \cdot \sum_i ([X_i] \cdot \hat{h}_i) + V \cdot \dot{T} \cdot \sum_i ([X_i] \cdot c_{p,i}(T)) \end{aligned} \tag{15}$$

Combining (12) and (15) and plugging (3) into the combination, the temperature rate, $\dot{T}$ is derived as follow:

$$\dot{T} = \frac{-\sum_i([\dot{X}_i]\cdot\hat{h}_i) - \dot{V}\cdot\sum_i([X_i]\cdot\hat{h}_i)/V + P\cdot\sum_i[\dot{X}_i]/\sum_i[X_i] - \dot{Q}/V}{\sum_i([X_i]\cdot c_{p,i}(T)) - P/T} \tag{16}$$

C. Chemical Kinetics

As can be seen from (3) and (16), other information, e.g. the values of $c_{p,i}$ and $\hat{h}_i$ as well as the history of species concentrations $[X_i]$, are required to solve these equations. This information can be obtained from the chemical kinetics part of the model, which is formed by the reaction mechanism.

Frist, several thermodynamic properties of each species, such as $c_{p,i}$ and $\hat{h}_i$, are functions of temperature T in the reaction mechanism via the NASA polynomial parameterization [37]:

$$\frac{c_{p,i}(T)}{R} = a_0 + a_1T + a_2T^2 + a_3T^3 + a_4T^4 \tag{17}$$

$$\frac{\hat{h}_i(T)}{RT} = a_0 + \frac{a_1}{2}T + \frac{a_2}{3}T^2 + \frac{a_3}{4}T^3 + \frac{a_4}{5}T^4 + a_5/T \tag{18}$$

where a_0 to a_5 are six parameters calibrated by NASA. To further reduce the computational cost, all the functions above are re-fitted into three order polynomial of T in the proposed model.

In addition, the history of each species concentration $[X_i]$ is derived via integrating the following differential equation:

$$[\dot{X}_i] = \frac{d}{dt}\left(\frac{N_i}{V}\right) = \frac{\dot{N}_i}{V} - \frac{\dot{V}N_i}{V^2} = w_i - \frac{\dot{V}}{V}[X_i] \tag{19}$$

where w_i is the production rate of species i from the reaction.

The heavy computational burden of the model with detailed chemical kinetics is usually caused by the tedious calculation processes, such as (17), (18) and (19). This burden is exacerbated significantly as the number of species and the number of reactions increase. In order to reduce the computational burden and keep sufficient chemical kinetics information, an engine operation cycle is separated into four phases (Fig. 4) and in each phase, a specific reaction mechanism with the minimal size is applied to predict the combustion process as precisely as possible:

Phase 1: this phase begins when piston locates at the BDC and ends when *T* reaches 500K. During this interval, few chemical reactions occur due to the low temperature and therefore, no reaction mechanisms need to be applied here.

Phase 2: A simplified reaction mechanism will be employed in this phase to represent the ignition process until all the fuel molecules are converted into intermediate species. Specifically in this model, methane (the major component of natural gas) is assumed as the fuel and the corresponding ignition mechanism is a one-step reaction converting all the methane into CO and H_2, as the intermediate species:

$$R_1 : CH_4 + 0.5O_2 \rightarrow CO + 2H_2$$

where its reaction rate is derived through the Jones-Lindstet mechanism (JL) [38]:

$$RR_1 = 4.4 \times 10^9 \cdot [CH_4]^{0.5} \cdot [O_2]^{1.25} \exp(-\frac{15095}{T}) \quad (20)$$

The corresponding production rate of each specie in this phase are:

$$\begin{cases} w_{CH_4} = -RR_1 \\ w_{O_2} = -0.5RR_1 \\ w_{H_2} = 2RR_1 \\ w_{CO} = RR_1 \\ w_{CO_2} = 0 \\ w_{H_2O} = 0 \end{cases} \tag{21}$$

For other fuels, specific reaction mechanisms for their ignition process can be found [39-41]. By applying those mechanisms, the proposed control-oriented model can be extended to different fuels.

Phase 3: afterwards, the intermediate species CO and H_2 will react to generate final products CO_2 and H_2O as well as to release the major of thermal energy. The corresponding reaction mechanism utilized in this phase is shown as below:

$$R_2 : CO + H_2O \rightarrow CO_2 + H_2$$
$$R_3 : H_2 + 0.5O_2 \rightarrow H_2O$$

where the reaction rates for both reaction steps are determined respectively [38, 42]:

$$RR_2 = 2.75 \times 10^7 \cdot [CO] \cdot [H_2O] \exp(-\frac{10065}{T}) \tag{22}$$

$$RR_3 = 1.5 \times 10^9 \cdot [H_2][O_2]^{0.5} \exp(-\frac{17609}{T}) \tag{23}$$

Similarly, the production rates of each species in this phase are the sum of all involved reaction rates:

$$\begin{cases} w_{CH_4} = 0 \\ w_{O_2} = -0.5RR_3 \\ w_{H_2} = RR_2 - RR_3 \\ w_{CO} = -RR_2 \\ w_{CO_2} = RR_2 \\ w_{H_2O} = -RR_2 + RR_3 \end{cases} \tag{24}$$

Sub-phase: when the temperature is over 1800K, the production of NOx should be taken into account. The thermal NOx generation mechanism [43] is added here since it is the most suitable mechanism for high temperature and rich oxygen environment. By kinetic analysis, an overall expression for the rate of thermal NOx formation is derived and modified from Bowman et al [44]:

$$w_{NO_x} = \frac{2.0 \times 10^{15}}{T^{0.5}} [N_2][O_2]^{0.5} \exp(\frac{-69090}{T}) \tag{25}$$

Phase 4: after the in-cylinder temperature *T* decreases to 900K, almost all the reaction products remain constants. Therefore, there is no need to consider the chemical kinetics any further and the rest of the cycle will be simulated as ideal expansion process with the heat transfer until the piston reaches the BDC again. It is also possible that not all the fuel molecules are consumed due to the relatively low temperature or extremely fuel-lean condition. In this case, phase 3 cannot be triggered and the process enters phase 4 directly.

To validate the boundary selection of the proposed separation method, simulations of two cases using the detailed GRI 3.0 mechanism are conducted. One case triggers combustion at CR = 31, Ω= 1.0 and equivalence air-fuel ratios AFR = 2.0. The other one is pure motoring process along the same piston trajectory.

As can be seen in Fig. 5, when the temperature is less than 500 K, the two temperature profiles are almost identical showing that the criterion for phase 1 is reasonable.

Also, the species concentration profiles of CH_4 and CO_2 in the combustion case are shown in Fig. 6.

As can be seen, most of the production of CO_2 starts right after the time instant when all the CH_4 has been consumed, which supports the criterion of phase 2.

Fig. 7 shows the species concentration profiles of NO, NO_2 and N_2O, respectively. The three species are produced after the temperature is over 1800K, which is the criterion to separate the sub-phase in phase 3.

In addition, the simulation also shows that all the species concentration are almost fixed after 30ms. Looking back to Fig. 5, the in-cylinder temperature at this time instant is about 1044 K in the combustion case. Thus, it is reasonable to assume that after the temperature decreases to 900K, all the reactions are frozen.

To summarize, the phase separation method transforms the entire chemical kinetics of the HCCI combustion into a sequence based on the thermal state, e.g. temperature, and the species concentration. Such a sequence guarantees the specific chemical kinetics in one phase has little effects on the simulation of the other phases. As a result, by applying the specific reaction mechanism in each phase, the proposed model not only increases the computational speed (30% in this study) by avoiding computing the entire chemical kinetics simultaneously, but also reduces the order of the control-oriented model, which facilitates the subsequent optimization process.

By now, the complete state space of the control-oriented model, e.g. pressure P, temperature T and each species concentration $[X_i]$, has been derived through (3), (16) and (19).

SIMULATION RESULT AND DISCUSSION

The simulation results of the proposed model are shown in this section and compared with the outcomes of three existing models, namely a simplified model [30], a reduced-order model and a detailed model [12]. The simplified model is developed based on the assumption that the entire chemical kinetics can be represented by a global reaction step reproducing the combustion of methane. Consequently, this model utilizes the integral of the Arrhenius reaction rate equation to predict the SOC timing. In addition, the subsequent heat release is assumed to be instantaneous after the combustion occurrence. The reduced-order model implements the Jones-Lindstet (JL) mechanism within the entire engine cycle to reproduce the combustion process of methane. As a benchmark for the proposed control-oriented model, the JL mechanism includes 4 reaction steps, which is similar to the proposed control-oriented model. The detailed model represents the chemical kinetics of methane through a detailed reaction mechanism, GRI-Mech 3.0 [45], and takes every elementary reactions into account. The development of the simplified model and the detailed model can be found in [30] and [12] respectively and the JL mechanism can be found in [38]. To have a fair comparison, initial conditions, in terms of air-fuel-ratio, thermal states of the intake air and piston trajectory profile, are fixed for the simulations of the four models.

A. Computational Cost

First of all, the computational cost of the four models are compared. The corresponding simulations are conducted using a laptop with 2.60GHz Inter(R) Core ™ i5-3230M processor and 4.00 GB installed memory.

As shown in Table. 1, the detailed model needs 2070ms to simulate an engine cycle, which only lasts 40ms. The reduced order model (with JL mechanism), on the other hands, spends only 134ms, which decreases the computational time by 93.5% compared to the detailed one. Obviously, such a significant reduction of computational time is mainly due to the lower order of the employed reaction mechanisms. As a detailed mechanism, the GRI-Mech 3.0 mechanism consists of 325 reactions, while the JL mechanism has four reaction steps. Furthermore, the proposed model requires even less time, 98ms, for the simulation of one engine cycle. Since the number of the reaction steps included in the reaction mechanism are similar to the reduced order model, such a 25 % improvement of the computational speed is achieved mainly by the unique phase separation methods developed in this study. Obviously, the improvement can be more significant if long-chain hydrocarbon fuels or renewable fuels are applied in the proposed model. However, the simplified model only takes 7ms to reproduce the combustion process within an engine cycle, which is still far beyond the other three.

B. Accuracy of the Prediction

Another comparsion of these models is the accuracy of the model predictions of HCCI combustion in terms of in-cylinder gas temperature profiles and NOx productions.

As shown in Fig. 8, the simulation result from the proposed model has a good agreement with the detailed model, which demonstrates its effectiveness. Both models predict similar peak temperature (2444K for the detailed model and 2442K for the proposed model) and SOC timing (20.06ms for detailed model and 19.97ms for proposed model). The performance of the reduce order model is acceptable to some extent, while its peak temperature (2495K) and SOC timing (19.65ms) slightly differ from the detailed model. On the other hand, the simplified model fails to represent the combustion precisely with over-estimated peak temperature (2601K) and SOC timing (20.48ms) due to the over-simplified chemical kinetics: the global reaction step neglects the heat release of the reactions occurring at low temperature, which causes the late prediction of the SOC timing. Additionally, due to the assumptions that the entire chemical energy is released instantaneously, the temperature rise in the simplified model is much greater than reality since the heat loss during the combustion process and the possibility of the incomplete combustion are ignored.

Besides, both the simplified model and the reduced order model cannot provide any information on NOx emission. As shown in Fig. 9, even though the NOx generation is only considered after the in-cylinder temperature reached 1800K in the proposed model, its final production of NOx still resembles the outcome of the detailed model. Such phenomenon attribute to the unique characteristic of the thermal NOx mechanism, which can be decoupled from the general combustion processes [45]. However, the critical information about the NOx emission is totally lost in the simplified model since the global reaction step only involves the fuel consumption.

Hence, despite of the least computational cost, the simplified model is not suitable for the control objective due to its discrepancy in the prediction of the combustion process and lack of information on emission production. On the other hand, the proposed control-oriented model offers a good balance between the computational cost and the accuracy of prediction, therefore makes itself a suitable candidate for control and optimization of the piston trajectory-based HCCI combustion control.

C. Comparison at Different Working Conditions

As the power source for automobiles or other mobile applications, the FPE should function adequately under the entire operation domain. Additionally, by applying the piston trajectory-based HCCI combustion control, the FPE is expected to operate at various CRs as well as different piston motion patterns between the TDC and BDC points, as shown in Fig. 3. Therefore, the proposed control-oriented model is required to sustain good agreement with the detailed model at various working conditions. In this subsection, both simulation results of the proposed model and the detailed model are compared herein, which effectively shows the fidelity of the proposed model at various working conditions. Inspired by Fig. 3, the simulation results are mainly categorized into two groups: 1. Various CR and 2. Different piston motion patterns, indicated by Ω.

1. Various CR

The simulation results of the two models are compared at a range of CR, from 28 to 39. Lower CR raises challenge for the ignition of methane under a fuel-lean HCCI condition and higher CR is avoided by the limitation of the physical strength of the material.

Various AFRs are also shown herein to reflect different load conditions. Three parameters are selected to demonstrate the accuracy of the prediction between these two models, e.g. the peak temperature T_{peak}, the SOC timing and the final NOx production. Fig. 10 to Fig. 12 show the relative error of these three terms respectively.

As shown in Fig. 10, the relative error of the T_{peak} is in the range of -15% to 3%. However, if the range of applied CR is narrowed from 30 to 39, the range of relative errors can be decreased from -5% to 3%. Obviously, the performance of the proposed control-oriented model is affected at the lower CR and higher AFR. After the CR drops to 28 and the AFR raises over 3, the ignition of the air-fuel mixture falls into a boundary condition, while the occurrence of the combustion is quite sensitive to the temperature and the species concentrations. Thus, one needs to be cautious to use the control-oriented model to simulate the combustion process in those working conditions.

Fig. 11 shows the relative error of the SOC timing between the proposed model and the detailed model. The range of the relative error of SOC timing is from -4% to 5%. Similar to the prediction of the T_{peak}, the performance of the proposed model is even better at high CR and lower AFR (relative error range from -1% to 2%). Besides, the overall relative error of SOC timing is smaller than the counterpart of the T_{peak}, which reveals the fact that the proposed model can precisely capture the combustion phasing at different working conditions. This information is critical since the combustion phasing of the HCCI combustion plays a key role in the control of the HCCI engine.

The comparison of the NOx emission between these two models is illustrated in Fig. 12. Obviously, the same trend of the NOx emissions is produced via the two models and the orders of magnitude of the results are similar as well. Since the NOx production is quite sensitive to the in-cylinder temperature, the agreement between the two models is reduced at high CRs due to the aggressive in-cylinder temperature rise accordingly. Besides, various AFRs influence the chemical kinetics of the NOx production due to the available chemical heat release. Parameters adaption for (25) based on the AFR can be conducted to improve the performance of the proposed model on the prediction of the NOx emissions at different AFRs.

2. Different Ω

Fig. 13, Fig. 14 and Fig. 15 show the comparison of the two models on the aforementioned three terms at various piston motion patterns, i.e. Ω. The range of the selected Ω is from 0.75 to 2.0. It is obvious from Fig. 13, the performance of the proposed model drops when the AFR is higher and the Ω is smaller. Similar to the CR case, these two conditions make it more difficult to ignite the methane. Especially, the piston trajectory with smaller Ω shortens the residential time of the piston around the TDC point (Fig. 3), which decreases the high temperature duration of the engine cycle and inhibit the corresponding ignition process. To the contrary, piston trajectory with larger Ω promotes the ignition process and facilitates the methane combustion. As a result, the proposed model performs well under these conditions.

The comparison of the SOC timing in various Ω is show in Fig. 14. As can be seen, the range of the relative error is within -2% to 2.5%. In this case, the proposed model captures the combustion phasing precisely. Similar conclusion for the NOx emission of the proposed model at various Ω can be reached, as shown in Fig. 15.

D. Adjusting Combustion Phasing Through Piston Trajectory

One of the most challenging parts of HCCI implementation is the control of combustion phasing. In the FPE with the piston trajectory-based HCCI combustion control, the ultimate freedom of piston motion can be used as an additional control means to regulate combustion phasing. In this subsection, a searching process of the optimal piston trajectory enabling the desired combustion phasing is presented. Additionally, due to the lack of the crankshaft mechanism, the widely-used parameter CA50, which represents the HCCI combustion phase in the conventional ICE, is replaced by T50, representing the time instant when 50% fuel chemical energy has been released in this study.

As shown in Fig. 16, a single-input-single-output feedback loop is utilized to achieve the optimal Ω of the piston trajectory. The objective is to force the T50 locating at the TDC point in order to realize the ideal Otto cycle and reduce the ringing intensity. To achieve this objective, a heat release analyzer is developed in order to calculate the simulated T50. Afterwards, the error between the calculated T50 and the targeted value is sent to a PI controller and the adjustment of Ω is calculated. In this way, the new piston trajectory is generated and the corresponding error in the following cycle will be

reduced. It should be noted that the PI gains are first calibrated to achieve the best convergence performance and then kept constant in the rest of simulations.

The heat release analyzer calculate the chemical heat release by integrating the instantaneous heat release rate, which is obtained from the piston trajectory and the in-cylinder gas temperature and pressure [36]:

$$\dot{Q}_{HR} = \frac{\gamma}{\gamma - 1} \cdot P \cdot \dot{V} + \frac{1}{\gamma - 1} \cdot V \cdot \dot{P} - \dot{Q} \tag{26}$$

where γ is the heat capacity ratio of the in-cylinder gas, which is set as 1.31 [36] and $\dot{Q}$ is the heat transfer rate. Given the fuel injection amount and its lower heating value, the 50% chemical energy within the injected fuel can be calculated offline and set as a preset. In addition, by integrating the heat release rate, the accumulated heat release can be obtained. The T50 value is then recorded as the time instant when the accumulated heat release reaches the above preset threshold.

As shown in Fig. 17, when CR = 31, AFR = 2.0, the first piston trajectory, whose Ω = 3.0, triggers combusiton early than the TDC point which increases the ringing intensity significantly. Using the searching method described above, the Ω of the piston trajectories in following cycle is reduced from 3.0 to 1.9 and the T50 values are moving closer to the TDC point (Fig. 17). Hence, the control of the combustion phase is realized by adjusting the piston trajectory through Ω and the optimal piston trajectory, which locates T50 at the TDC point, is achieved eventually. The optimal piston trajectory is then sent to the detailed model and the comparison between the proposed model and the detailed model presents good agreement again.

The performance of the searching method is also investigated during the transient operations. As shown in Fig. 18, the left side of the green dashed line represents different working conditions with various AFRs under CR = 31 and the right side represents different working conditions with various AFRs under CR = 34. As can be seen, no matter how the CR or the AFR is changed, the searching method with the proposed model can always achieve an optimal Ω, realizing the desired combustion phasing, after 3 or 4 cycle's simulation, which only lasts 0.3 to 0.4s. As a comparison, the detailed model is also implemented into the searching method to determine the optimal Ω for the combustion phasing control. However, the turnaround time of this process is about 20s, which is far beyond the requirement for the real time application.

CONCLUSION

In this paper, a new control-oriented model with a unique phase separation method is developed to realize the trajectory-based HCCI combustion control. In order to reduce the computational burden and keep sufficient chemical kinetics information for HCCI combustion, the engine cycle is separated into four phases and in each phase, a specific reaction mechanism with the minimal size is applied. With the unique phase separation method, the proposed control-oriented model not only shows a good agreement with the detailed physical-based model, in terms of in-cylinder gas temperature and NOx emissions, but also reduces the computation time by 95%. In addition, such a good agreement is sustained at various working conditions, including different CRs, multiple AFRs and various piston motion patterns Ω. Meanwhile, an example for searching the optimal piston trajectory with the desired combustion phasing is shown. By using the

proposed model, the optimal piston trajectory can be achieved within 0.4s, which enables real time optimization of combustion phasing at variable working conditions. In the future, the framework of the proposed control-oriented model will be extended to other fuels, including renewable fuels. Additionally, optimal piston trajectories can be designed based on the proposed control-oriented model to maximize the extracted work output and minimize the emissions.

ACKNOWLEDGMENT

The study is supported in part by National Science Foundation (NSF) under grant CMMI-1634894

NOMENCLATURE

A	Major axis of the ellipse, m
A_{wall}	The surface area of the engine heat transfer, m^2
a_0 *to* a_5	Six parameters calibrated by NASA for thermal states of each species in the reaction mechanism
B	Location of the ellipse center as the bias, m
b	The bore of free piston engine, 79.5 mm
$C_{p,i}$	The mole-based constant pressure heat capacity of species *i, J/mol K*
f	Frequency of the engine operation, Hz
h	The specific enthalpy of the in-cylinder gas, J/kg
h_{hl}	The heat transfer coefficient, W/m^2K
$\hat{h}_i$	The mole-based specific enthalpy of species *i*, J/mol
m	The total mass in the cylinder, kg
N_i	The mole number of species *i*, mol
t	Time, s
P	The pressure of the in-cylinder gas, bar
$\dot{Q}$	The heat transfer rate, J/s
Q_{HR}	The rate of heat release during the combustion, J/s

R	The universal gas constant, 8.314 J/mol K
S	Piston Trajectory, m
T	The temperature of the in-cylinder gas, K
T_{wall}	The temperature of the engine wall, 500K
u	The specific internal energy of the in-cylinder gas, J/kg
V	The volume of the combustion chamber, m^3
v	The specific volume of the in-cylinder gas, m^3/kg
$\dot{W}$	The rate of expansion work, J/s
w	The average speed of the in-cylinder gas, 8 m/s
w_i	The production rate of species *i, mol/m³ s*
$[X_i]$	The concentration of species *i*, $Kmol/m^3$

Greek Letters

α	The architecture parameter of the FPE, 2
Υ	The heat capacity ratio of the in-cylinder gas, 1.31
Ω	The shape of the ellipse, representing the piston motion pattern

Acronyms

AFR	Equivalence ratio of air-fuel ratio, actual air-fuel ratio/stoichiometric air-fuel ratio
BDC	Bottom Dead Center

CR	Compression ratio
CA50	Crank Angle at 50% fuel burnt
FPE	Free piston engine
HCCI	Homogeneous charge compression ignition
ICE	Internal combustion engine
SOC	Start of combustion
T50	Time instant at 50% fuel burnt
TDC	Top dead center

REFERENCES

[1] Onishi, S.,Han Jo, S., Shoda, K., Do Jo, P. and Kato, S., 1979, "Active Thermo-Atmosphere Combustion (ATAC): A New Combustion Process for Internal Combustion Engine," SAT Technical Paper Series, Paper NO. 790501

[2] Zhao, F., Asmus, T. W., Assanis, D. N, and Dec, J. E., 2003, "Homogeneous Charge Compression Ignitions (HCCI) Engines: Key Research and Development Issues," SAE International, PT-94

[3] Epping, K., Aceves, S., Bechtold, R. and Dec, J., 2002, "The Potential of HCCI Combustion for High Efficiency and Low Emissions," SAE Technical Paper 2002-01-1923

[4] Zhao, H., Peng, Z., Williams, J., Ladommatos, N., 2001, "Understanding the Effects of Recycled Gases on the Controlled Autoignition (CAI) Combustion in Four-Stroke Gasoline Engines." SAE Paper No.2001- 01-3607

[5] Ladommatos, N. Abdelhalim, S, and Zhao, H., 2000, "The Effects of Exhaust Gas Recirculation on Diesel Combustion and Emissions," Int. J. Engine. Res., **1**(1), pp. 107–126

[6] Dec, J. E., 2002, "A Computational Study of the Effects of Low Fuel Loading and EGR on Heat Release Rates and Combustion Limits in HCCI Engines," SAE Paper NO. 2002-01-1309

[7] Caton, P. A., Songm H. H., Kaahaainam N. B. and Edwards, C. F., 2005, "Strategies for Achieving Residual-Affected Homogeneous Charge Compression Ignition using Variable Valve Actuation," SAE Paper NO. 2005-01-0165

[8] Caton, P. A., Simon, A. J., Gerdes, J. C., and Edwards, C. F., 2003, "Residual-Effected Homogeneous Charge Compression Ignition at Low Compression Ratio Using Exhaust Reinduction," Int. J. Engine Res., **4**(3), pp. 163–177

[9] Law, D., Kemp, D., Allen, J., Kirkpatrick, G., and Copland, T., 2001, "Controlled Combustion in an IC-Engine with a Fully Variable Valve Train," SAE Paper No. 2001-01-0251

[10] Marriott, C. D and Reitz, R. D., 2002, "Experimental Investigation of Direct Injection Gasoline for Premixed Compression Ignited Combustion Phasing Control," SAE Paper NO. 2002-01-0418

[11] Sjoberg, M., Edling, L. O., Eliassen, T., Magnusson, L. and Angstrom, H. E., 2002, "GDI HCCI: Effects of Injection Timing and Air-Swirl on Fuel Stratification Combustion and Emissions Formation." SAE Paper NO. 2002-01-0106

[12] Zhang, C., Li, K. and Sun, Z., 2015, "Modeling of Piston Trajectory-based HCCI Combustion Enabled by a Free Piston Engine," Applied Energy, 139(1), pp. 313-326

[13] Zhang, C. and Sun, Z., 2016, "Using Variable Piston Trajectory to Reduce Engine-out Emissions," Applied Energy, 170(1), pp. 403-313

[14] Zhang, C. and Sun, Z., 2017, "Trajectory-based Combustion Control for Renewable fuels in Free Piston Engines," Applied Energy, 187(1), pp. 72-83

[15] Li, K., Sadighi, A. and Sun, Z., 2014, "Active Motion Control of a Hydraulic Free Piston Engine," IEEE/ASME Transaction. Mechatronics, 19(4), pp. 1148-1159

[16] Mikalsen, R. and Roskilly, A. P., 2007, "A Review of Free-piston Engine History and Applications," Applied Thermal Engineering, 27(14-15), pp.2339-2352

[17] Li, K., Zhang, C. and Sun, Z., 2015, "Precise Piston Trajectory Control for a Free Piston Engine," Control Engineering Practice, 34, pp. 30-38

[18] Zhang, C. and Sun, Z., 2016, "Optimization of Trajectory-based HCCI Combustion," Proceedings of Dynamic Systems Control Conference, Minneapolis MN, 2016-9726

[19] Turanyi, T., 1990, "Sensitivity Analysis of Complex Kinetics Systems. Tool and Applications," J. Math. Chem., vol.5, pp. 203-244

[20] Turanyi, T., Berces, T. and Vajda, S., 1989, "Reaction Rate Analysis of Complex Kinetic Systems," Int. J, Chem. Kinet., vol.21, pp. 83-99

[21] Mass, U. and Pope, S. B., 1992, "Simplifying Chemical Kinetics: Intrinsic Low-Dimensional Manifolds in Composition Space," Proc. Combust. Inst., vol.24, pp. 103-112

[22] Lam, S. H. and Goussis, D. A., 1994, "The CSP Method for Simplifying Kinetics," Int. J. Chem. Kinet., vol.26, pp. 461-486

[23] Lu, T. and Law, C. K, 2005, "A Directed Relation Graph Method for Mechanism Reduction," Proc. Combust. Inst, vol.30, pp. 1333-1341

[24] Pepiot-Desjardins, P. and Pitsch, H., 2008, "An Efficient Error-Propagation-Based Reduction Method for Large Chemical Kinetic Mechanisms," Combust, Flame, vol.154, pp.67-81

[25] Ra, Y., and Reitz, R. D., 2008, "A Reduced Chemical Kinetics Model for IC Engine Combustion Simulations with Primary Reference Fuels," Combustion and Flame, 155, pp. 713-738

[26] Aceves, S. M., Martinez-Frias, J. Flowers, D., Smith, J. R., Dibble, R. and Chen, J. Y., 2002, "A Computer Generated Reduced Iso-octane Chemical Kinetic Mechanism Applied to Simulation of HCCI Combustion," SAE Technical Paper Series, 2002-01-2870

[27] Jia, M. and Xie, M., 2006, "A Chemical Kinetics Model of Iso-octane Oxidation for HCCI Engine," Fuel, 85, pp. 2593-2604

[28] Toulson E., Allen, C. M. and Miller D. J., 2011, "Modeling the Autoignition of Fuel Blends with a Multistep Model," Energy and Fuels, 25(2), pp. 632-639

[29] Shaver, G. M. Gerdes, J. C. Jain, P., Caton, P. A. and Edwards, C. F., 2003, "Modeling for Control of HCCI Engines," Proceeding of American Control Conference, Denver, CO, 2003

[30] Li, K. and Sun, Z., 2011, "Stability Analysis of a Hydraulic Free Piston Engine with HCCI Combustion," Proceedings of Dynamic Systems Control Conference, Arlington VA, 2011

[31] Zhang, S., Song, R. and Zhu, G. G., 2017, "Model-based Control for Model Transition Between Spark Ignition and HCCI Combustion," Journal of Dynamics Systems, Measurement and Control, 139(4), 041004

[32] Yang, X. and Zhu, G. G., 2011, "a Two-zone Control Oriented SI-HCCI Hybrid Combustion Model for the HIL Engine Simulation," Proceedings of 2011 American Control Conference, San Francisco, CA, 2011

[33] Shahbakhti, M. and Koch, C. R., 2010, "Physics Based Control Oriented Model for HCCCI Combustion Timing," Journal of Dynamics Systems, Measurement and Control, 132(2), 021010

[34] Karagiorgis, S., Collings, N., Glover, K. and Petridis, T., 2006, "Dynamic Modeling of Combustion and Gas Exchange Processes for Controlled Auto-ignition Engines," Proceedings of 2006 American Control Conference, Minneapolis, MN, 2006

[35] Shaver, G. M., Gerdes, J. C., Roelle, M. J., Caton, P. A. and Edwards, C. F, 2005, "Dynamic Modeling of Residual-affected Homogeneous Charge Compression Ignition Engines with Variable Valve Actuation," Journal of Dynamics Systems, Measurement and Control, 127, pp. 374-381

[36] J. Heywood, 1988, Internal Combustion Engine Fundamentals, McGraw-Hill

[37] Goodwin, D., Malaya N. and Speth. R., "Cantera: An Object-oriented Software for Chemical Kinetics, Thermodynamics and Transport Processes", available at https://code.google.com/p/cantera/

[38] Jones, W. P. and Lindstedt, R. P., 1988, "Global Reaction Schemes for Hydrocarbon Combustion," Combustion and Flame, 73(3), pp. 233-249

[39] Westbrook, C. K. and Dryer, F. L., 1980, "Simplified Reaction Mechanisms for the Oxidation of Hydrocarbon Fuels in Flames," Combustion Science and Technology, 27(1-2), pp. 31-43

[40] Yamada, H., Sakanashi, H., Choi, N., and Tezaki, A., 2013, "Simplified Oxidation Mechanism of DME Applicable for Compression Ignition," SAE Technical Paper 2003-01-1819

[41] Zeppieri, S. P., Klotz, S. D., and Dryer, F. L., 2000, "Modeling Concepts for Larger Carbon Number Alkanes: a Partially Reduced Skeletal Mechanism for N-decane Oxidation and Pyrolysis," Proceedings of the Combustion Institute, 28(2), pp. 1587-1595

[42] Wang, L., Liu, Z., Chen, S. and Zheng, C., 2012, "Comparison of Different Global Combustion Mechanisms under Hot and Diluted Oxidation Condition," Combust. Sci. Technol., 184(2), pp. 1-18, 2012

[43] Zeldovich, Y. A., Frank-Kamenetskii, D. and Sadovnikov, P., 1947, "Oxidation of Nitrogen in Combustion," Publishing House of the Academy of Sciences of USSR

[44] Bowman, C. T., 1975, "Kinetic of Pollutant Formation and Destruction in Combustion," Progress in Energy Combust. Sci., 1(1), pp. 33-45

[45] Smith, G. P., Golden, D. M., Frenklach, M., Moriarty, N. W., Eiteneer, B., Goldenberg, M., Bowman, C. T., Hanson, R. K., Song, S., Gardiner Jr, W. C., Lissianski, V. V. and Qin, Z., http://www.me.berkeley. edu/gri_mech/

[46] Zhang, C., Li, K. and Sun, Z., 2015, "A Control-oriented Model for Piston Trajectory-based HCCI Combustion Control Enabled by Free Piston Engines," Proceeding of the American Control Conference, Chicago, IL 2015

Figure Captions List

Table Caption List

Table 1 Comparison of the computational times of four models

Table. 1 Comparison of the computational times of four models

Utilized model	**Computation time [ms]**
Detailed model	2070
Reduced order model	134
Proposed model	98
Simplified model	6

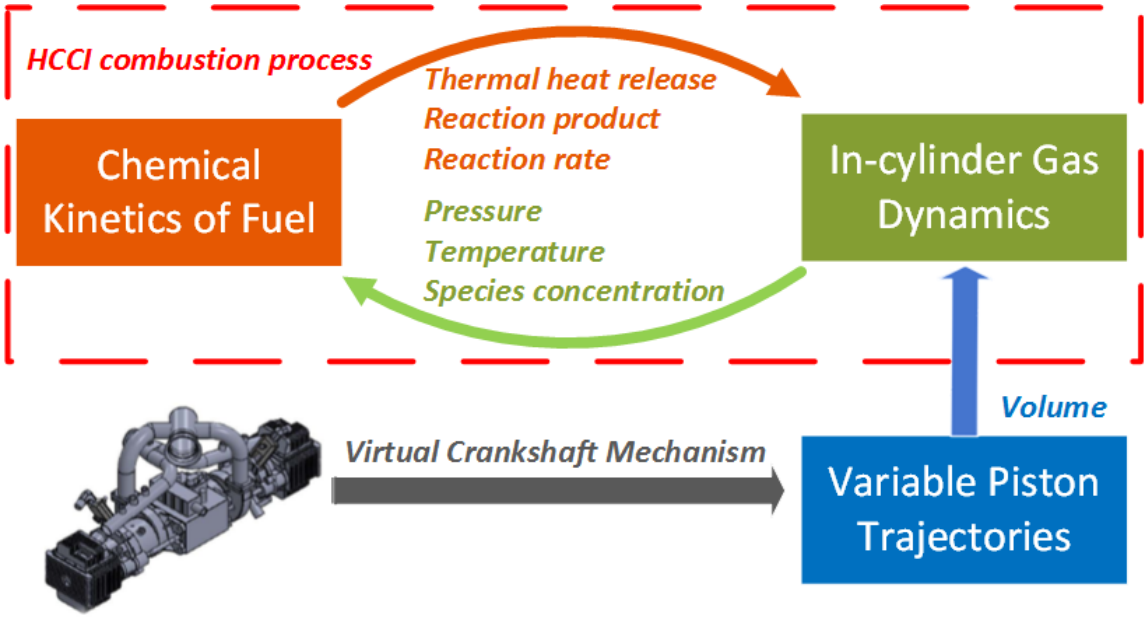

Fig. 1 Interaction between chemical kinetics and gas dynamics

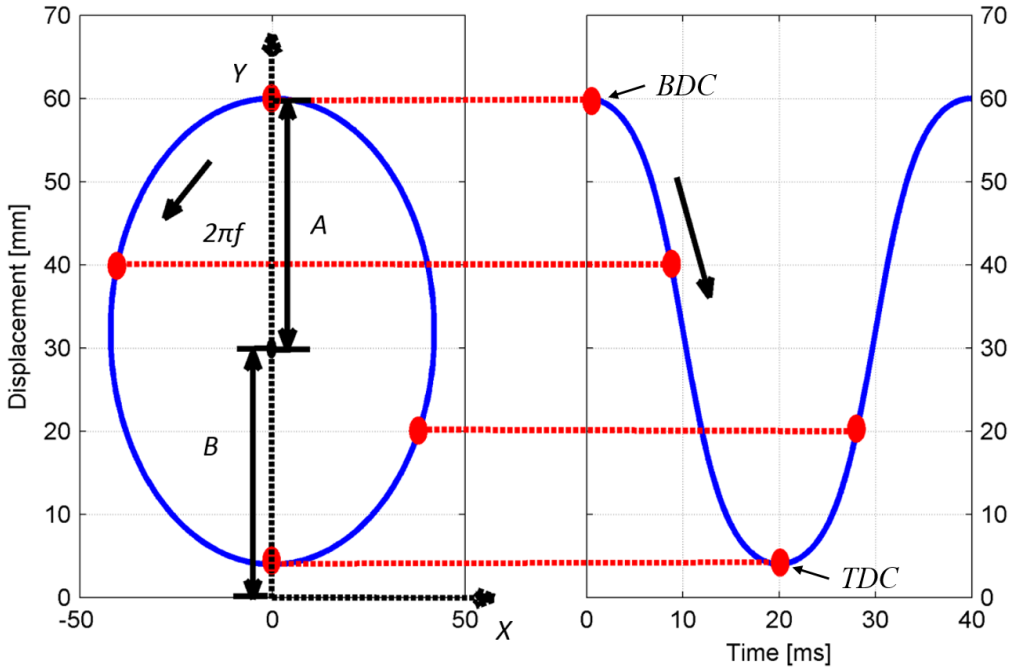

Fig. 2 Description of FPE piston motions

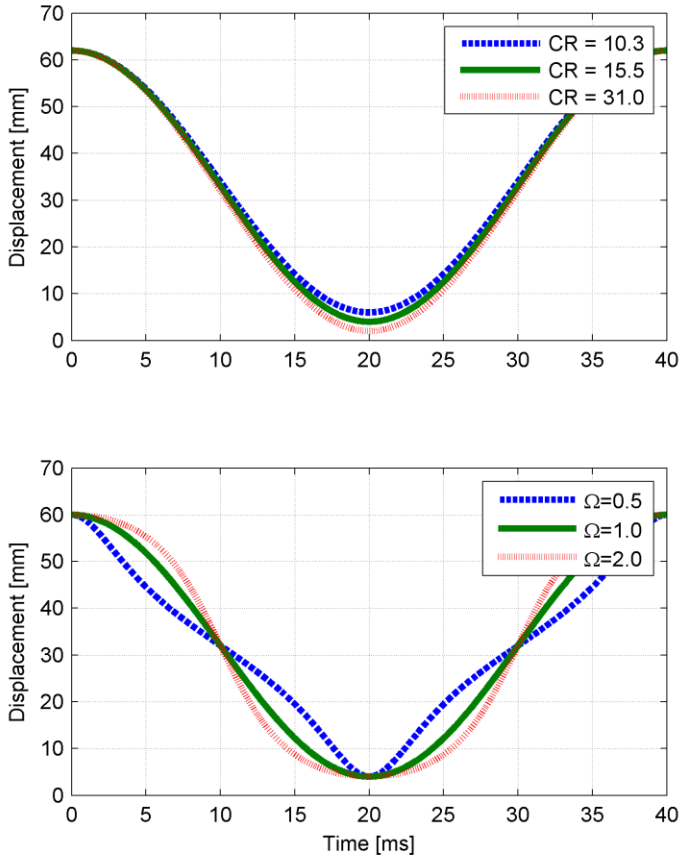

Fig. 3 Piston trajectories with different CR (top) and Ω (bottom)

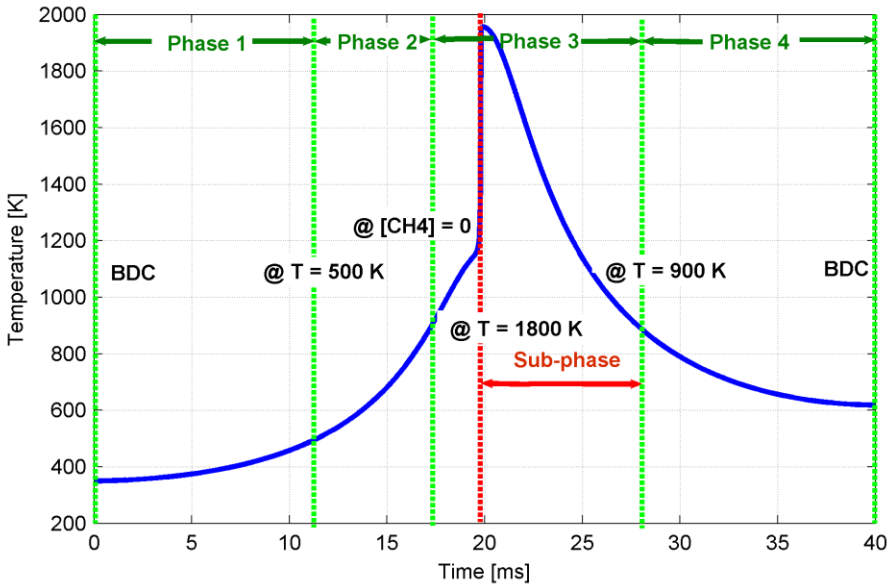

Fig. 4 Phase separation within an engine cycle

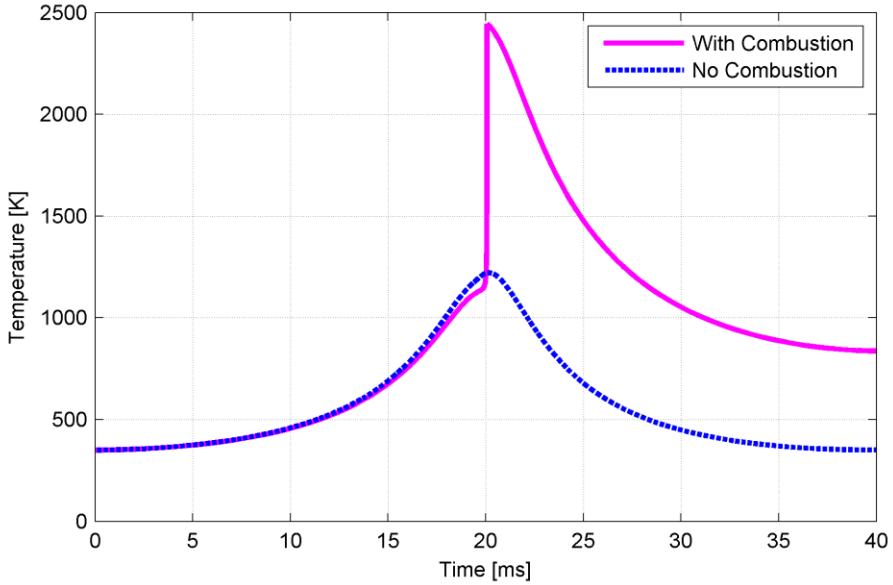

Fig. 5 Comparison between the combustion and motoring processes along the same piston trajectories

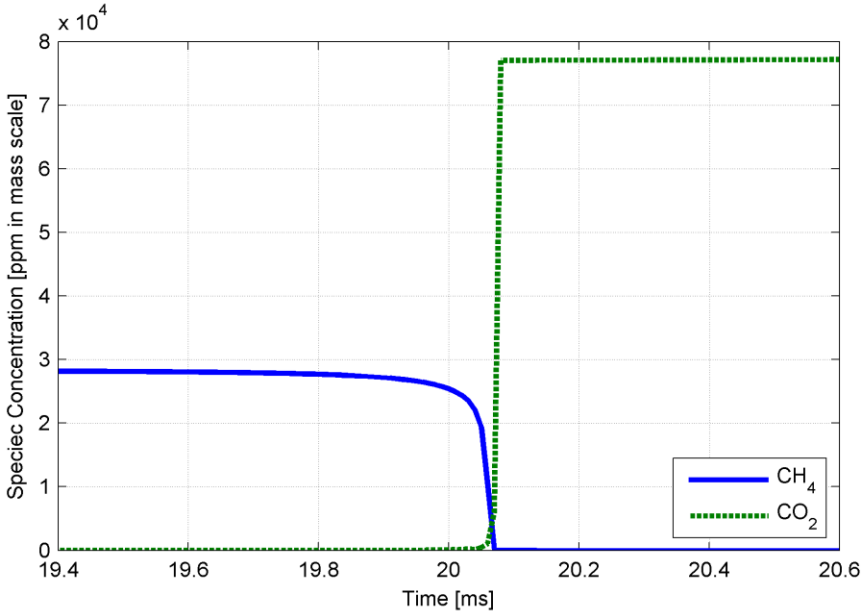

Fig. 6 CH_4 and CO_2 species concentration profiles during the combustion process

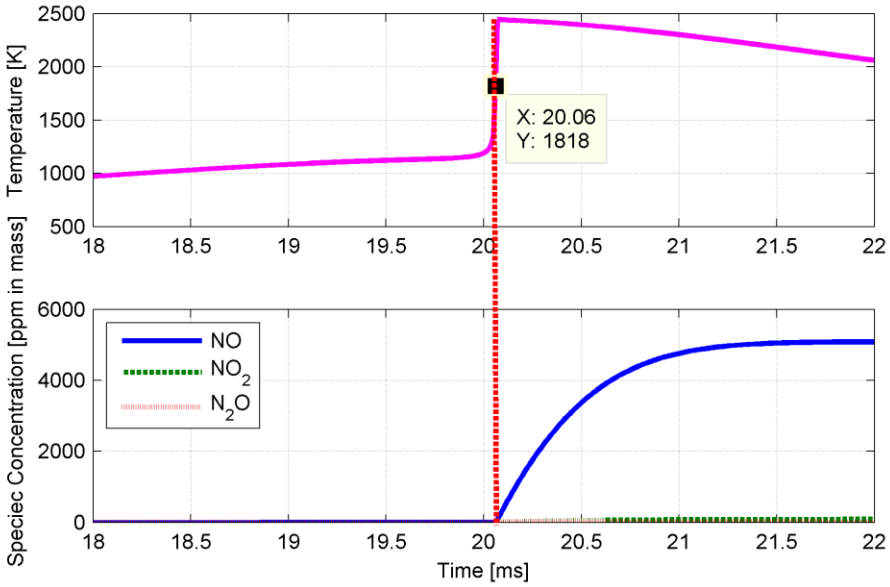

Fig. 7 NO, N_2O and NO_2 species concentration and temperature profiles during the combustion process

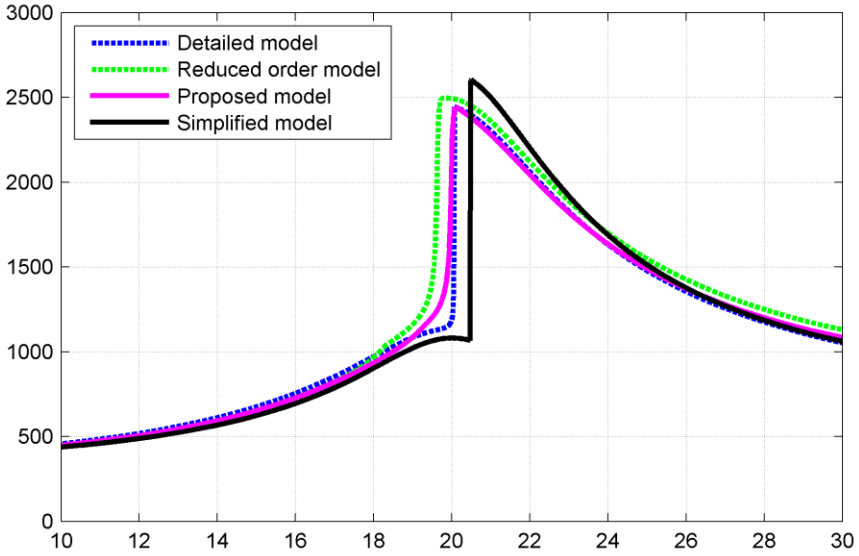

Fig. 8 Comparison of temperature profiles from four models (AFR = 2, CR = 31 and Ω =1)

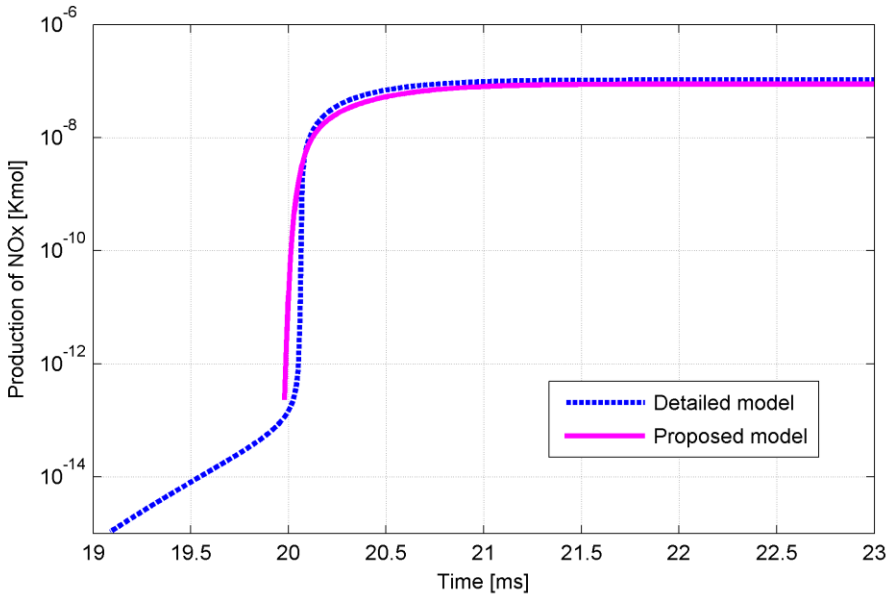

Fig. 9 Comparison of NOx production from the two models (AFR = 2, CR = 31 and Ω =1)

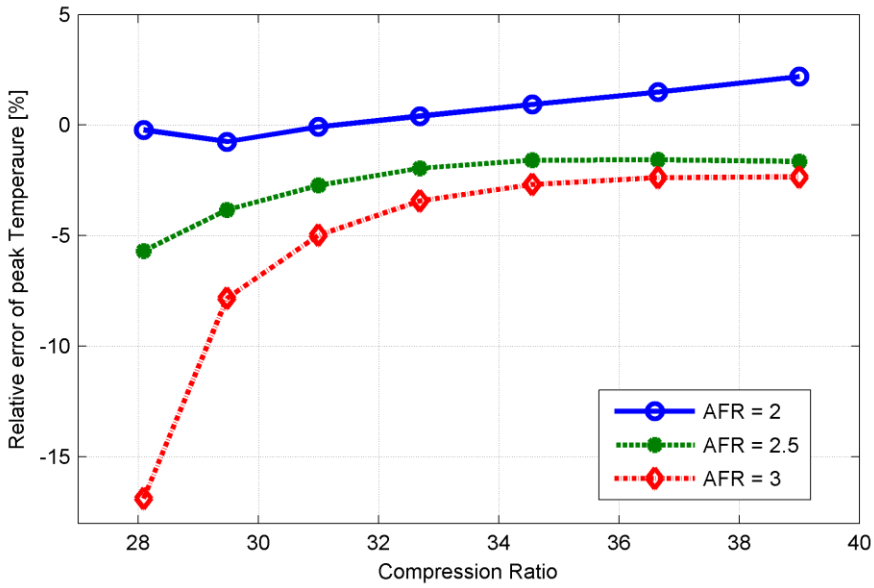

Fig. 10 Relative error of peak Temperature from the two models at various CRs and different AFRs

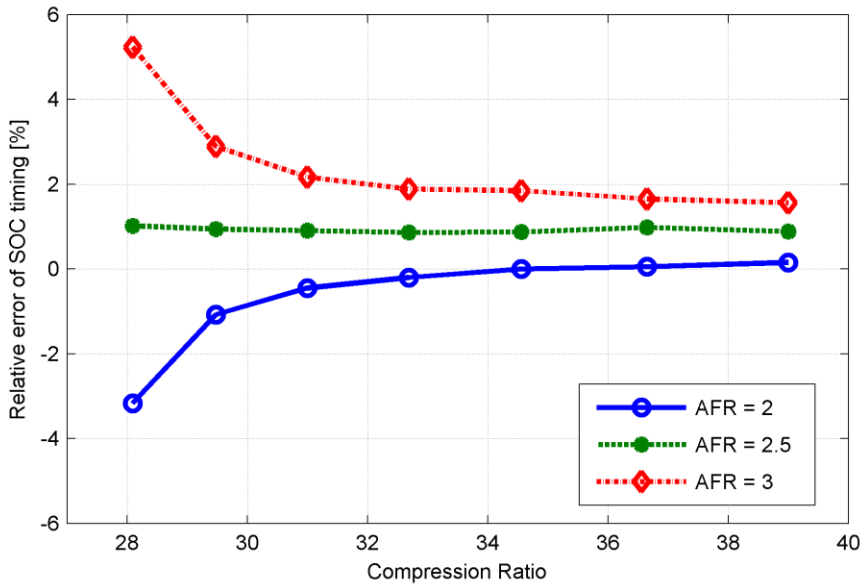

Fig. 11 Relative error of SOC timing from the two models at various CRs and different AFRs

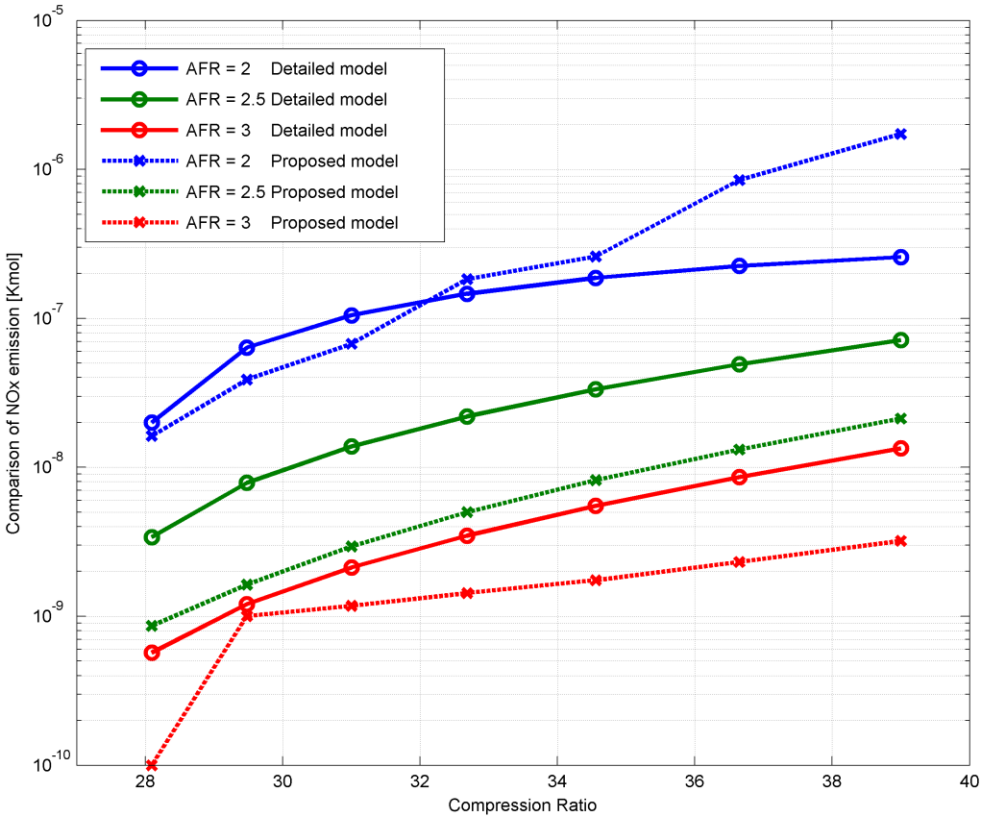

Fig. 12 Comparison of NOx production from the two models at various CRs and different AFRs

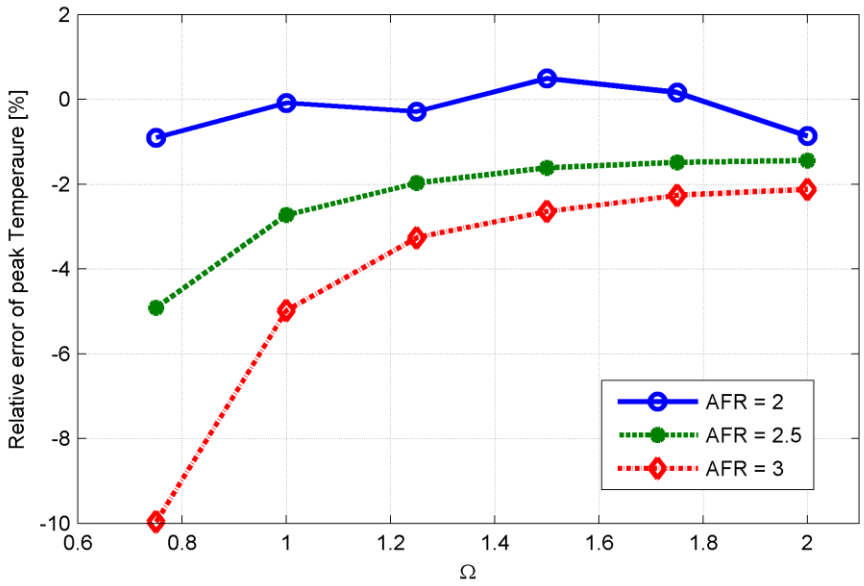

Fig. 13 Relative error of peak Temperature from the two models at various Ωs and different AFRs

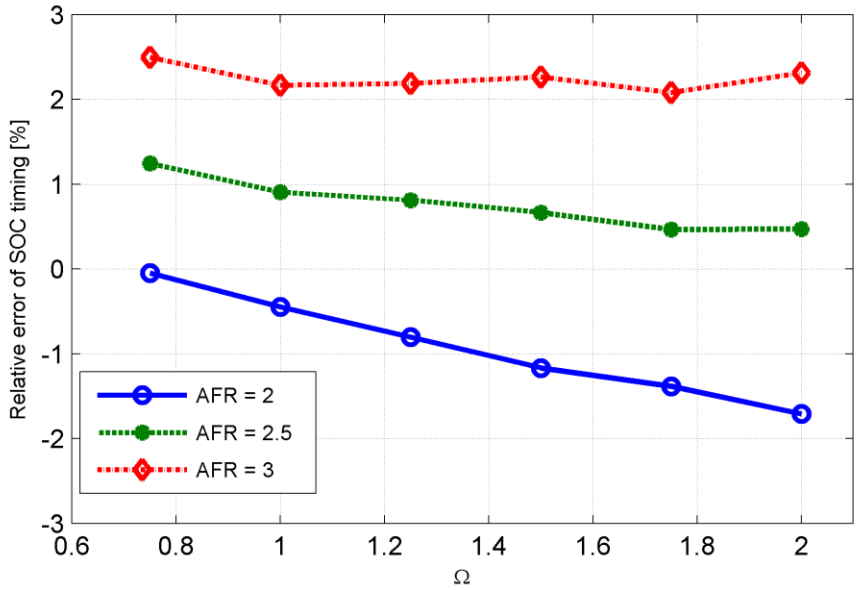

Fig. 14 Relative error of SOC timing from the two models at various Ωs and different AFRs

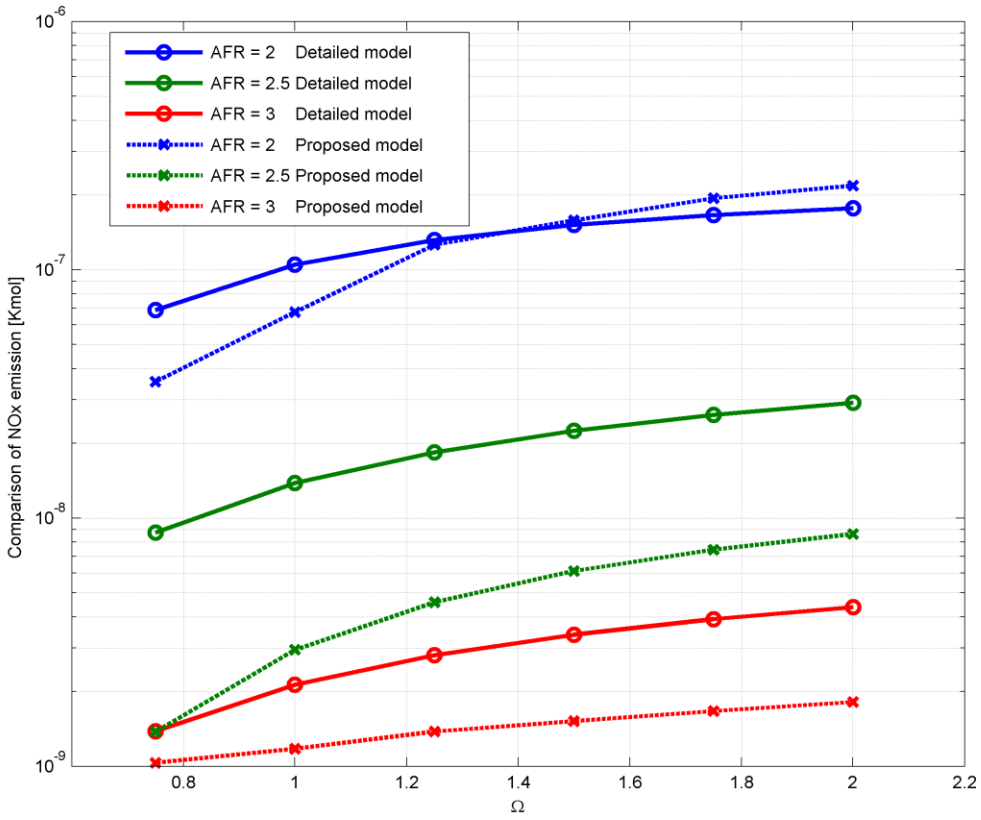

Fig. 15 Comparison of NOx production from the two models at various Ωs and different AFRs

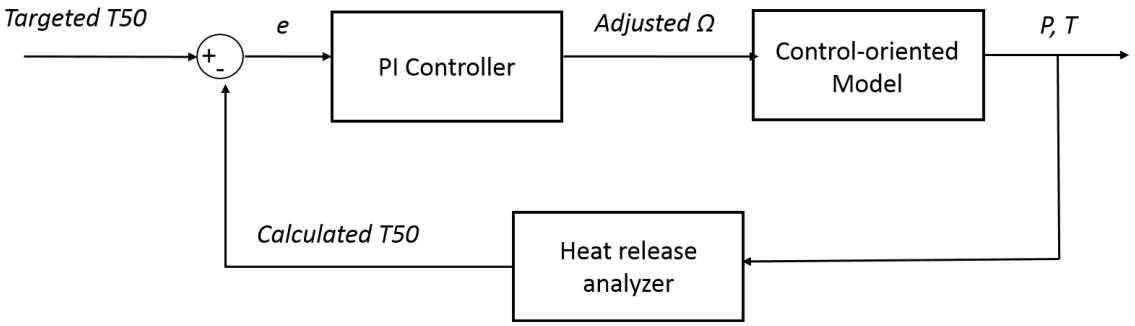

Fig. 16 Block diagram of the feedback loop searching the optimal piston trajectory with desired combustion phasing

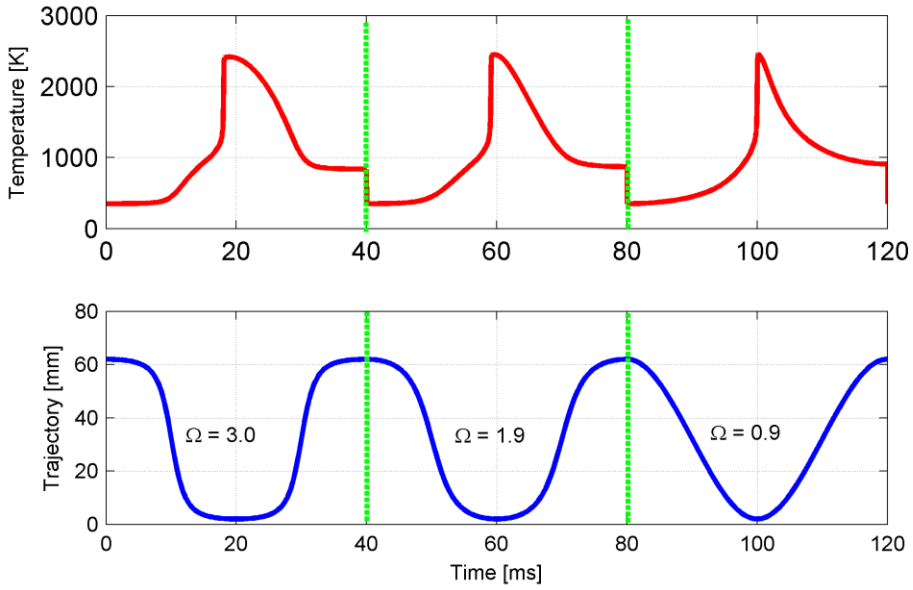

Fig. 17 Searching process for the optimal piston trajectory (AFR = 2, CR = 31)

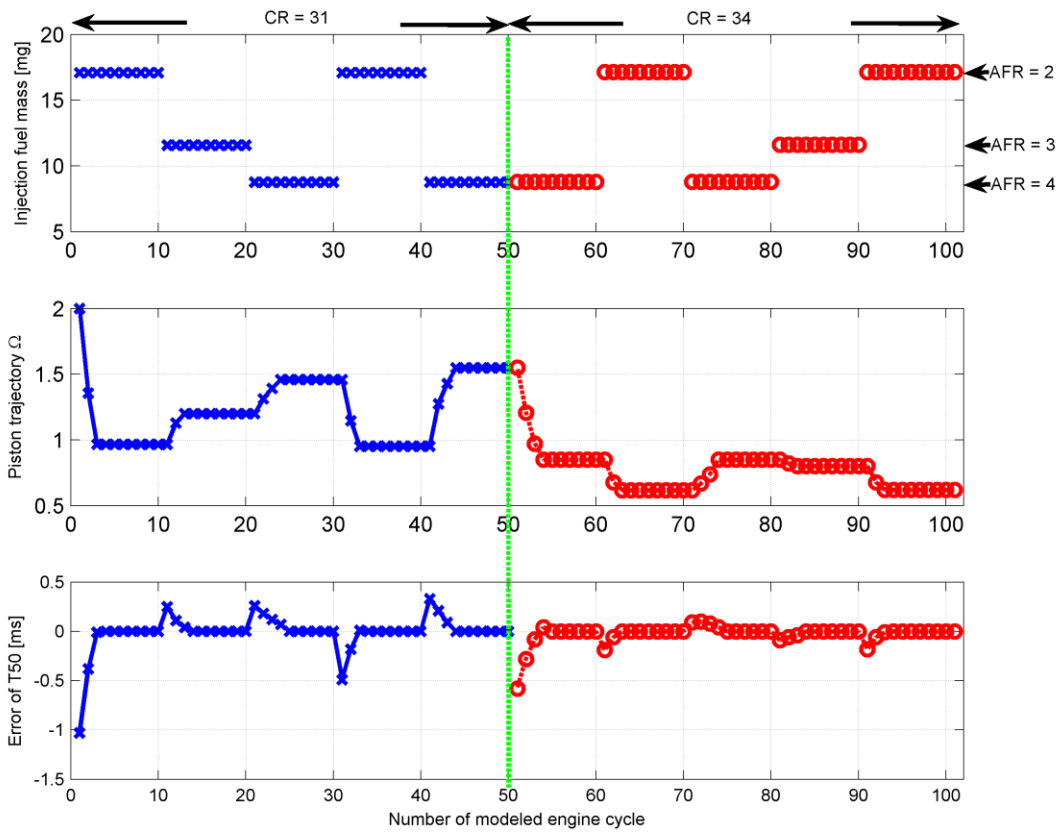

Fig. 18 Searching process of the optimal piston trajectories during the transient operations (various CRs and AFRs)